Research

Hormone-control regions mediate steroid receptor–dependent genome organization

François Le Dily,[1,4] Enrique Vidal,[1,4] Yasmina Cuartero,[1,2] Javier Quilez,[1,5] A. Silvina Nacht,[1] Guillermo P. Vicent,[1,6] José Carbonell-Caballero,[1] Priyanka Sharma,[1] José Luis Villanueva-Cañas,[1] Roberto Ferrari,[1] Lara Isabel De Llobet,[1] Gaetano Verde,[1,7] Roni H.G. Wright,[1] and Miguel Beato[1,3]

[1]*Gene Regulation, Stem Cells and Cancer Program, Center for Genomic Regulation (CRG), The Barcelona Institute of Science and Technology, Barcelona 08003, Spain;* [2]*CNAG-CRG, Center for Genomic Regulation (CRG), The Barcelona Institute of Science and Technology, Barcelona 08028, Spain;* [3]*Universitat Pompeu Fabra (UPF), Barcelona 08002, Spain*

In breast cancer cells, some topologically associating domains (TADs) behave as hormonal gene regulation units, within which gene transcription is coordinately regulated in response to steroid hormones. Here we further describe that responsive TADs contain 20- to 100-kb-long clusters of intermingled estrogen receptor (ESR1) and progesterone receptor (PGR) binding sites, hereafter called hormone-control regions (HCRs). In T47D cells, we identified more than 200 HCRs, which are frequently bound by unliganded ESR1 and PGR. These HCRs establish steady long-distance inter-TAD interactions between them and organize characteristic looping structures with promoters in their TADs even in the absence of hormones in ESR1$^+$-PGR$^+$ cells. This organization is dependent on the expression of the receptors and is further dynamically modulated in response to steroid hormones. HCRs function as platforms that integrate different signals, resulting in some cases in opposite transcriptional responses to estrogens or progestins. Altogether, these results suggest that steroid hormone receptors act not only as hormone-regulated sequence-specific transcription factors but also as local and global genome organizers.

[Supplemental material is available for this article.]

The folding of the eukaryotic chromatin fiber within the cell nucleus, together with nucleosome occupancy, linker histones, and post-translational modifications of histones tails, plays an important role in modulating the function of the genetic information. It is now well demonstrated that the genome is nonrandomly organized in a hierarchy of structures, with chromosomes occupying territories that are partitioned into segregated active and inactive chromatin compartments (Cavalli and Misteli 2013; Gibcus and Dekker 2013; Fraser et al. 2015). Furthermore, chromosomes are segmented into contiguous "topologically associating domains" (TADs), within which chromatin interactions are more frequent than with the neighboring regions (Dixon et al. 2012; Nora et al. 2012; Sexton et al. 2012). Such organization has been shown to participate in DNA replication and transcription (Cavalli and Misteli 2013; Pope et al. 2014; Lupianez et al. 2015). Boundaries between TADs are conserved among cell types and are enriched for cohesins and CTCF binding sites, as well as for highly expressed genes. However, how boundaries are established and maintained is not yet fully understood (Hou et al. 2012; Jin et al. 2013; Dixon et al. 2015). TADs are further organized in subdomains and loops that also depend on CTCF and other factors linked to transcription regulation (Phillips-Cremins et al. 2013; Dowen et al. 2014; Rao et al. 2014). The sub-TAD organization is more divergent between cell types, and it dynamically reorganizes during the process of differentiation (Phillips-Cremins et al. 2013; Ji et al. 2016). In terminally differentiated cells, it remains unclear whether TADs are relatively stable preorganized structures or whether they are dynamically remodeled in response to transient external cues (Jin et al. 2013; Seitan et al. 2013; Le Dily et al. 2014; Kuznetsova et al. 2015). Nevertheless, it is now accepted that TADs facilitate contacts between gene promoters and their regulatory elements located far away on the linear genome (Sanyal et al. 2012; Dowen et al. 2014; Zhan et al. 2017). However, it is not clear to what extent cell-specific transcription factors modulating the activity of those regulatory sites are also involved in organizing this particular level of chromatin folding.

Steroid receptors are stimuli-induced transcription factors that regulate the expression of thousands of genes in hormone responsive cells (Cicatiello et al. 2004; Bain et al. 2007; Ballare et al. 2013). Notably, the estrogen and progesterone receptors (ESRs and PGRs, respectively) are known to bind either directly to the promoter of their target genes or to enhancer elements where they orchestrate the recruitment of chromatin remodeling complexes and general transcription factors (Carroll et al. 2005; Hsu et al. 2010; Ballare et al. 2013; Li et al. 2013). Several studies have analyzed the effects of steroids on the 3D organization of chromatin at limited resolution, leading to apparently contradictory results. For example, we previously showed that TADs can respond as units to the hormone signals with dynamic reorganization of the entire TAD

[4]These authors contributed equally to this work.
Present addresses: [5]Bioinformatics, Clarivate Analytics, Barcelona 08025, Spain; [6]Centro de Biología Molecular Severo Ochoa, CSIC-UAM, 28049 Madrid, Spain; [7]Department of Basic Sciences, Universitat Internacional de Catalunya, Barcelona 08017, Spain
Corresponding author: miguel.beato@crg.es
Article published online before print. Article, supplemental material, and publication date are at http://www.genome.org/cgi/doi/10.1101/gr.243824.118.

(Le Dily et al. 2014). In contrast, other studies suggested that enhancers and promoters contacts precede receptor activation (Hakim et al. 2009; Jin et al. 2013). These scenarios are not mutually exclusive, and it is possible that different regulatory mechanisms are required depending on the general chromatin context (Kuznetsova et al. 2015).

Results

The TAD encompassing the *ESR1* gene is organized around an HCR

In a previous study with T47D breast cancer cells, we observed that TADs can behave as units of response to steroid hormones (Le Dily et al. 2014). One of these steroid-responsive TADs contains the *ESR1* gene (encoding the ESR1 protein) and five other protein-coding genes, which are coordinately up-regulated by estradiol (E2) and down-regulated by progestins (Pg) (Supplemental Fig. S1A; Le Dily et al. 2014). To study at high resolution the organization of this domain (hereafter referred to as *ESR1*-TAD), we designed capture enrichment probes covering a 4-Mb region of Chromosome 6, including the *ESR1*-TAD (Fig. 1A). These probes were used in Capture-C experiments to generate contact maps at various resolutions from cells grown in conditions depleted of steroid hormones (Fig. 1A,B). We used these data sets to create virtual 4C profiles, taking as baits the promoters of protein coding genes laying in *ESR1*-TAD (Supplemental Fig. S1B). We observed that in addition to establishing contacts between them, promoters were engaged in frequent interactions with a 90-kb intergenic region located upstream of the *ESR1* gene promoter (Fig. 1B; Supplemental Fig. S1B). Similarly, virtual 4C profile tacking as bait the whole 90-kb intergenic region confirmed that it engaged interactions with virtually all upstream and downstream promoters of protein coding genes as well as with other nonannotated sites marked by H3K4me3 and RNA-Polymerase II (RNA Pol II) within the boundaries of *ESR1*-TAD (Fig. 1C). This 3D organization of the *ESR1*-TAD was confirmed in an independent Capture Hi-C experiment (Supplemental Fig. S1C).

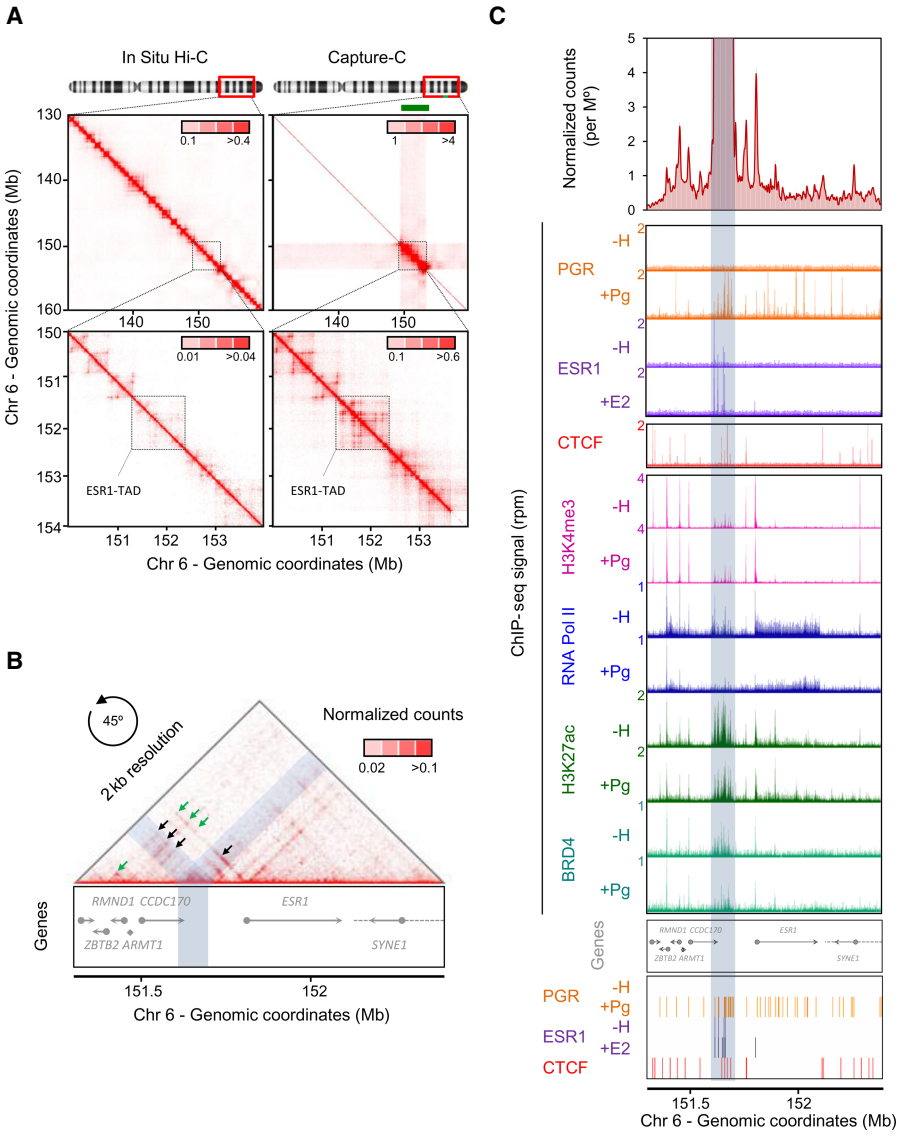

Figure 1. The *ESR1*-TAD is organized around an HCR. (*A, top*) Normalized contact maps at 100-kb resolution of a 30-Mb region of Chr 6 encompassing the *ESR1*-TAD (Chr 6: 130,000,000–160,000,000) in T47D cells before (in situ Hi-C; *left*) or after capture enrichment (*right*) with biotinylated probes directed against the region marked in green (Chr 6: 149,750,000–153,750,000). (*Bottom*) Magnification at 10-kb resolution of the 4-Mb region containing the *ESR1*-TAD (dashed square). Color scales in *insets* correspond to the normalized count numbers per million of genome-wide valid pairs. (*B*) Contact matrix at 2-kb resolution of the *ESR1*-TAD (Chr 6: 151,300,000–152,400,000; the matrix was rotated 45°, and the top half is shown). Green arrows highlight the loops established between promoters; black arrows, between promoters and the 90-kb intergenic region. Color scales in *insets* correspond to the normalized counts number per million of genome-wide valid pairs. (*C, top*) Virtual 4C profile at 2-kb resolution (expressed as normalized counts per million within the region depicted) using the 90-kb intergenic region (highlighted in blue) as bait. Panels *below* correspond to Genome Browser tracks of ChIP-seq reads per million (rpm) profiles obtained for the different factors and epigenetic marks listed in the absence (−H) or presence of progestin (+Pg) or estradiol (+E2). Positions of protein coding genes; position of significant CTCF, ESR1, and PGR binding sites in the presence or absence of hormones; as well as genomic coordinates are shown at the *bottom*.

Chromatin immunoprecipitation (ChIP)-seq data obtained from T47D cells exposed to E2 or Pg demonstrated that this 90-kb region is enriched in hormone-induced ESR1- and PGR-associated chromatin sites (Fig. 1C; Supplemental Fig. S1D). In absence of steroids (−H), ESR1 but not PGR was already bound to chromatin at four sites within the region (Fig. 1C; Supplemental Fig. S1D). Exposure of cells to E2 (+E2) increased ESR1 binding at the preexisting sites, and only one site was bound de novo by the hormone-activated ESR1 (Fig. 1C; Supplemental Fig. S1D). Upon treatment with Pg (+Pg), PGR bound to about 40 different locations distributed throughout the *ESR1*-TAD (Fig. 1C). Among those sites, 12 were concentrated within the 90-kb intergenic region that

contacts all promoters (Fig. 1C; Supplemental Fig. S1D). This region was further characterized by the expression of several nonannotated transcripts, which, similarly to the nearby protein-coding genes, were oppositely regulated by E2 and Pg (Supplemental Fig. S1E,F; Le Dily et al. 2014), as well as by high density of RNA Pol II, BRD4, H3K4me3, and H3K27ac (Fig. 1C). Upon exposure to Pg and binding of the PGR, the levels of H3K27ac, BRD4, and RNA Pol II decreased within the region (Fig. 1C; Supplemental Fig. S1G) in correspondence with the decreased expression of the genes in this condition (Supplemental Fig. S1A).

Together, these observations indicate that, in the absence of steroids, the *ESR1*-TAD is organized around a 90-kb intergenic region where ESR1 is already bound in an unliganded form and where both ESR1 and PGR cluster after exposure to their cognate ligand. Such a region probably coordinates the hormone-induced changes in transcription of the genes within *ESR1*-TAD, and we therefore designate it as a hormone-control region (HCR).

HCRs participate in organizing the T47D genome

In order to generalize these observations, we used ChIP-seq data sets of ESR1 and PGR in T47D cells exposed to E2 or Pg to identify potential HCRs genome-wide. Applying the detection scheme depicted in Figure 2A (see also the Methods section and Supplemental Fig. S2A,B), we identified a total of 2681 regions enriched mainly in PGR binding sites (PGR ≥ 3; ESR1 < 3), 164 enriched mainly in ESR1 binding sites (PGR < 3; ESR1 ≥ 3), and 212 putative HCRs enriched in both ESR1- and PGR-associated chromatin sites (PGR ≥ 3; ESR1 ≥ 3). These HCRs were located in TADs containing genes related with hormone-responsive mammary cell identity, for example the *PGR* gene as well as *FOXA1* (Fig. 2A). In steroid-depleted conditions, these HCRs, of a median size of 30 kb, were characterized by high levels of FOXA1 binding, as well as by enhancer associated marks (e.g., H3K27ac, BRD4, and RNA Pol II) compared with their flanking regions (Fig. 2B). Although HCRs were defined based on the number of binding sites after exposure to the hormones, they were frequently characterized by binding of unliganded receptors (Fig. 2C). In hormone-depleted conditions, 78% and 53% of the HCRs were already occupied at one or more site(s) by unliganded ESR1 or PGR, respectively (Fig. 2C). The steroid deprivation protocol of 2.5 d used in this study led to the loss of ~50% of the ESR1 binding sites observed in complete growing conditions (Supplemental Fig.

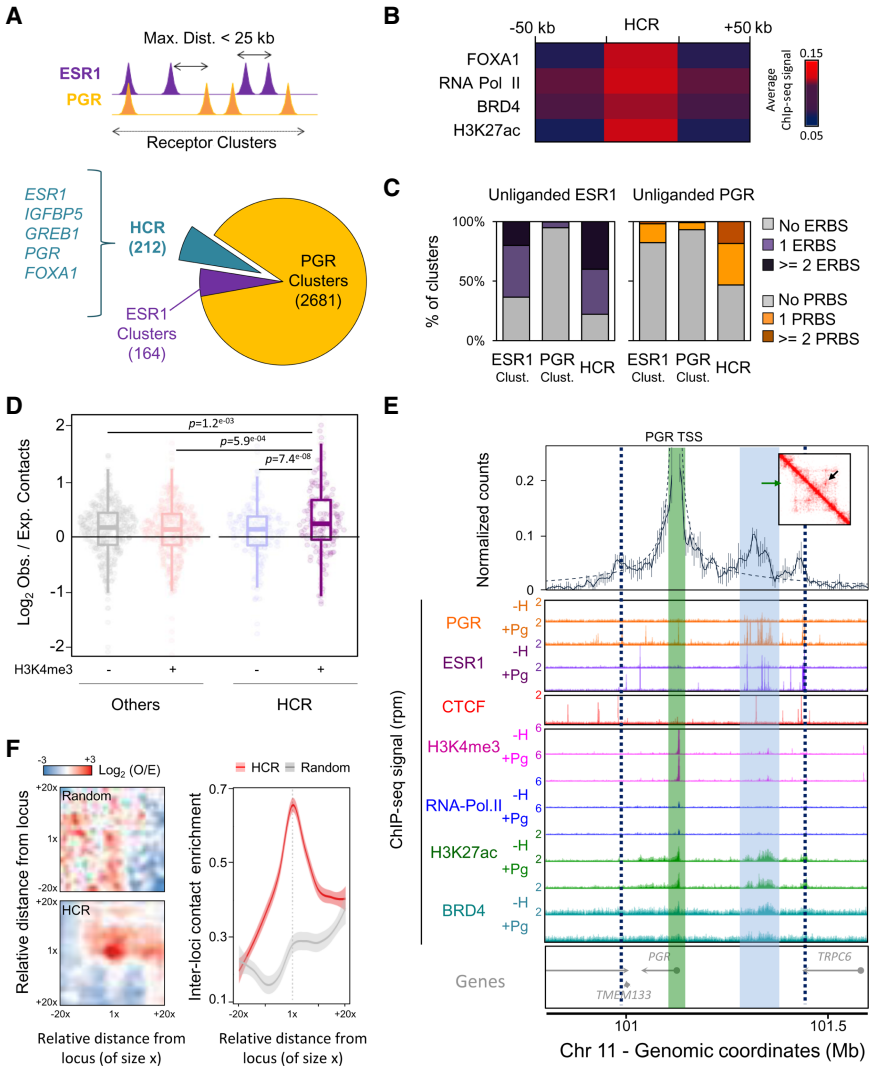

Figure 2. Genome-wide characterization of HCRs. (*A*) Strategy used to identify clusters of receptor binding sites (also see Methods section and Supplemental Fig. S2A). The pie chart indicates the number of clusters of each type. Examples of genes of interest found in TADs harboring an HCR are shown on the side. (*B*) Average ChIP-seq signal of specific factors and marks in HCRs and their flanking regions (±50 kb upstream or downstream). (*C*) Percentage of cluster (either ESR1-predominant, PGR-predominant, or HCRs) exhibiting zero, one, or more than one binding site for ESR1 (ERBS; *left*) or PGR (PRBS; *right*) in cells maintained in conditions depleted of steroid hormones (unliganded ESR1 or PGR). (*D*) Distribution of observed versus expected intra-TAD interactions established between HCRs or non-HCRs regions (others) with loci marked (+) or not (–) by H3K4me3. *P*-values of differences between the different groups are shown (Student's *t*-test). (*E*, *top*) Virtual 4C profile at 5-kb resolution using the TSS of *PGR* (highlighted in green) as bait (average ± SD of two independent in situ Hi-C experiments). The position of the largest HCR detected in this region is highlighted in blue. The *inset* shows the corresponding in situ Hi-C contact matrices obtained in T47D cells grown in the absence of hormones. The green arrow shows the position of the TSS of *PGR*, and the black arrow points to the loop established between the promoter and the HCR. Panels *below* correspond to Genome Browser tracks of ChIP-seq profiles obtained for the different factors and epigenetic marks listed in absence (–H) or presence of progestin (+Pg) or estradiol (+E2). Positions of protein coding genes as well as genomic coordinates are shown at the *bottom*. Borders of the *PGR*-TAD are marked with a dashed blue line. (*F*) Analysis of the long-range inter-TADs interactions established between HCRs (HCR–HCR) or between random regions of similar sizes and separated by similar distances. (*Left*) The *x*-axis and *y*-axis correspond to the relative genomic coordinates considering the region of interest (of size *x*) as center. Color scale reflects the observed versus expected contacts (also see Methods section). (*Right*) Graph corresponds to the average (± confidence interval) signal observed at the loci of interest (red, HCR-HCR contacts; gray, random-random contacts).

S2C). No major additional loss is observed even after 12 d of culture in absence of steroids (Supplemental Fig. S2C), showing that a 2.5-d withdrawal of steroids is sufficient to erase the majority of the sites occupied by hormone-activated receptors. This suggests that the remaining chromatin-associated ESR1 sites correspond to unliganded receptor binding sites, which may correspond to memory sites important for further response to the hormones.

To determine whether these HCRs corresponded to long-range regulatory elements as observed in the case of the *ESR1*-TAD, we generated in situ Hi-C samples from T47D cells grown in steroid-depleted conditions (Supplemental Table S1). We computed the frequencies of contacts of the identified HCRs within their host TADs and observed that they more frequently established intra-TAD interactions with sites marked by H3K4me3 (active promoters) than with other loci (Fig. 2D). HCR-H3K4me3 contacts occurred at higher frequency than contacts between H3K4me3 sites and other loci within the TAD, supporting the potential role of HCRs in controlling gene expression (Fig. 2D). For example, such interactions were observed between the promoter of *PGR* gene and the HCRs detected in its TAD (Fig. 2E). We also used the in situ Hi-C data to measure the frequency of contacts between HCRs located >2 Mb apart within the same chromosome. We observed a significant tendency of long-range HCR–HCR intra-chromosomal contacts compared with the contacts between random regions of similar sizes separated by similar distances (Fig. 2F). Together these observations point toward a regulatory and structural role of HCRs in the absence of hormones not only at the TAD scale but also at higher levels of chromosomal organization.

Differences in the structural organization of TADs in ESR1$^+$/PGR$^+$ and ESR1$^-$/PGR$^-$ breast cells correlate with HCR occupancy by the receptors

ChIP-seq experiments of ESR1 and PGR in MCF-7 cells showed that despite the very different levels of ESR1 and PGR (Supplemental Fig. S3A) and despite the limited overlap between ESR1 and PGR binding sites between the two breast cancer cell lines (Supplemental Fig. S3B), ESR1 and PGR also cluster in regions corresponding to the HCRs identified in T47D in this other cell line. Notably, out of the 212 HCRs identified in T47D cells, 62 (29.2%) were classified as such in MCF-7 cells (PGR $\geq$ 3; ESR1 $\geq$ 3), and 118 (55.7%) were also enriched in ESR1 binding sites in these cells (Supplemental Fig. S3C). For example, the E2-induced binding of ESR1 to the *ESR1*-TAD HCR at sites already occupied in hormone-depleted conditions was also observed in MCF-7 cells (Supplemental Fig. S3D). Upon exposure to Pg, PGR also binds to the *ESR1*-TAD HCR in MCF-7. However, this binding occurs at sites mainly overlapping with the ESR1 binding sites and thus different from the PGR binding sites observed in T47D (Supplemental Fig. S3D). In T47D cells, binding of ESR1 and PGR in HCRs occurred frequently at nonoverlapping sites (Supplemental Fig. S3E). In contrast, there was a higher overlapping between the binding sites of the two receptors in MCF-7 cells within the same regions (Supplemental Fig. S3E). Thus, despite qualitative and quantitative differences in the position of individual binding sites, it appears that clustering of ESR1 and PGR occurs in similar regions in different ESR1$^+$/PGR$^+$ cell lines, supporting a functional role of HCRs in breast cancer cells.

By comparing independent in situ Hi-C replicates generated from ESR1$^+$-PGR$^+$ breast cancer cell lines (T47D, MCF-7, and BT474) and in ESR1$^-$-PGR$^-$ cells (MCF10A and SKBR3), all grown in absence of hormones (Supplemental Table S1), we observed that regions identified as HCRs in T47D were also engaging long-range interactions between them in the ESR1$^+$-PGR$^+$ breast cancer cell lines but neither in the ESR1$^-$-PGR$^-$ ones nor in the ESR1$^-$-PGR$^-$ lymphoblastoid cell line GM12878 (Fig. 3A). These HCR regions were also engaged in frequent interactions with sites marked by H3K4me3 within their own TAD in ESR1$^+$-PGR$^+$ but not in ESR1$^-$-PGR$^-$ cell lines (Fig. 3B). For instance, when we compared the organization of the *ESR1*-TAD in the different cell lines, we observed structural differences that suggested higher similarities between cells of the same steroid receptor status (Supplemental Fig. S4A–D). The main structural differences corresponded to the HCR interactions, which did not establish contacts with the promoters in ESR1$^-$-PGR$^-$ cells (Supplemental Fig. S4C,D). Similarly, in the absence of hormone, the promoter of the *PGR* gene is establishing contacts with the HCR in the three ESR1$^+$-PGR$^+$ cell lines but not in the ESR1$^-$-PGR$^-$ ones (Fig. 3C–E; Supplemental Fig. S4E–G). These observations support the notion that HCRs organize the intra-TAD contacts as well as higher levels of genome structure in ESR1$^+$-PGR$^+$ cells. In addition, our results suggest that the binding of the receptors, in particular ESR1 (Fig. 2C; Supplemental Fig. S3D), might be responsible for the cell-specific organization of HCR-containing TADs between ESR1-PGR-expressing and -nonexpressing cells.

Hormone-independent binding of steroid receptors at HCRs participates in the maintenance of a functional TAD organization

The binding pattern of CTCF is highly similar in ESR1$^+$-PGR$^+$ and ESR1$^-$-PGR$^-$ cells (Supplemental Fig. S5A). Both in T47D and GM12878, CTCFs bound at TAD borders engage in stronger interactions between them compared with CTCFs located within TADs (Supplemental Fig. S5B). In T47D, HCRs engage in stronger interactions with the promoters located within their TAD than CTCF-bound sites do (Supplemental Fig. S5B). Such interactions of the regions corresponding to HCRs are not observed in GM12878 where ESR1 and PGR are absent (Supplemental Fig. S5B). For instance, the majority of the CTCF binding sites located within the *ESR1*-TAD are shared between T47D and GM12878 cells (Supplemental Fig. S5C). However, as mentioned above and confirmed in Capture Hi-C experiments, the interactions between promoters and the *ESR1*-TAD HCR were strikingly different between the two cell types (Supplemental Fig. S5D-F), notably with sites bound by ESR1 in absence of hormone involved in apparent CTCF-independent looping with the promoters (Supplemental Fig. S5D–F).

Since the functional interactions of HCRs were observed in absence of steroids in cells expressing ESR1 and PGR, we wondered whether the fractions of unliganded receptors bound to chromatin could directly participate in the maintenance of such organization in the absence of hormones. To test this hypothesis, we knocked-down ESR1 expression in T47D cells by transient transfection with siRNA against *ESR1* (siRNA-*ESR1*). In two independent transient transfection experiments, a mild decrease (45%) of the levels of ESR1 in siRNA-*ESR1*–transfected cells was accompanied by a concomitant decrease of the level of *PGR* transcripts in hormone-depleted conditions (Fig. 4A,B). This was accompanied by a decrease of the interactions between the *PGR* promoter and the HCR in siRNA-*ESR1*–transfected cells compared with cells transfected with scramble siRNA (siRNA-Control) (Fig. 4C,D). Similarly, we observed a decrease in the interactions between HCRs and promoters within the *ESR1*-TAD (Fig. 4E). Although modest, comparable trends were observed in T47D cells, where PGR levels were

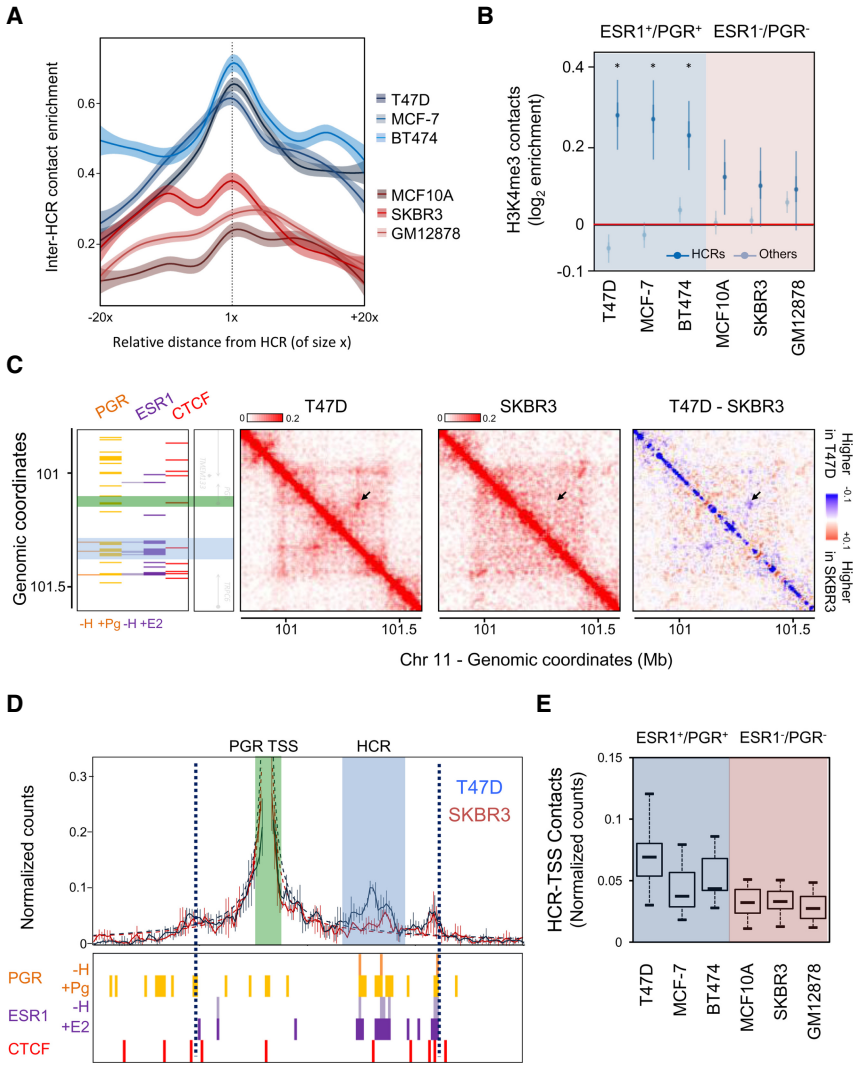

Figure 3. Internal structures of HCR-containing TADs correlate with ESR1/PGR status. (*A*) Analysis of long-range inter-TAD interactions established in different cell lines between regions corresponding to the HCRs defined in T47D. The graph shows the average (± confidence interval) of contacts between HCRs located at >2 Mb using HCRs as in Figure 2F (red lines, ESR1$^-$-PGR$^-$ cell lines; blue lines, ESR1$^+$-PGR$^+$ cell lines). (*B*) Distributions of observed versus expected intra-TAD interactions established between the HCRs identified in T47D with loci marked by H3K4me3 in the different ESR1$^+$-PGR$^+$ and ESR1$^-$-PGR$^-$ cell lines analyzed (dark blue bars). The light blue bars correspond to the observed versus expected intra-TAD interactions established between non-HCR loci with loci marked by H3K4me3 in the same TADs. (*) *P*-values <0.01 in pair-wise comparisons of the two distributions for each cell line (paired *t*-test). (*C*) Normalized in situ Hi-C contact matrices at 5-kb resolution over the *PGR*-TAD (Chr 11: 100,800,000–101,600,000) obtained in T47D (as in Fig. 2E) and SKBR3 cells (color-scaled according to the normalized counts per thousand in the region depicted). The difference between the contact matrices is shown on the *right* with blue and red corresponding to contacts higher and lower in T47D than in SKBR3, respectively. Positions of protein coding genes; position of significant CTCF, ESR1, and PGR binding sites in the presence or absence of hormones (–H, +Pg, +E2); and genomic coordinates are shown on the *left*. Positions of the TSS of *PGR* and its nearby HCR are highlighted in green and blue, respectively. The black arrow points the loop established between the HCR and the promoter in T47D cells. (*D*) Virtual 4C profiles at 5-kb resolution (average ± SD of two biological replicates) obtained using the promoter of *PGR* as bait in T47D (blue) or SKBR3 (red). Position of CTCF, ESR1, and PGR binding sites in presence or absence of hormones (–H, +Pg, +E2) are shown at the *bottom*. The positions of the TSS of *PGR* and its nearby HCR are highlighted in green and blue, respectively. Borders of the *PGR*-TAD are marked with a dashed blue line. (*E*) Distribution of contacts between genomic bins within the HCR with the TSS of *PGR* in the different cell lines.

knocked-down by shRNA (Verde et al. 2018). Indeed, in situ Hi-C performed in shEmpty or shPGR cells also suggested a differential organization of the *ESR1*- and *PGR*-TADs, with the interactions between HCRs and promoters partially disrupted in shPGR cells (Supplemental Fig. S6A,B). In this case, this effect might be related to the decrease in PGR levels and/or to the concomitant decreased expression of ESR1 protein levels in shPGR cells (Verde et al. 2018).

Together these observations support the hypothesis that steroid receptors bound to chromatin in absence of ligand serve to organize and maintain HCRs interactions with promoters prior to the exposure, potentially to favor further response to hormones.

HCR-containing TADs are dynamically restructured upon exposure to hormones

To further interrogate the functional role of the identified HCRs, we generated in situ Hi-C from T47D cells exposed to Pg or E2 for 30 or 180 min (Supplemental Table S1). The long-range inter-TAD interactions between HCRs were mainly maintained upon exposure to the hormones (Fig. 5A). However, when we analyzed the Pg-induced modifications of enhancer-associated marks at HCRs in T47D cells, we noticed that distinct populations of HCRs could be separated based on the hormone-induced changes in BRD4 signal (Fig. 5B; Supplemental Fig. S7A). Seventy loci showed enhanced recruitment of BRD4 upon exposure to Pg, correlating with increased H3K27ac and RNA Pol II levels (Supplemental Fig. S7A); we refer to these HCRs as HCR$^+$ (Fig. 5B). On the other hand, exposure to Pg decreased the level of these marks in 71 HCRs, which we refer to as HCR$^-$ (Fig. 5B). We thus calculated the global transcriptional changes that occur within HCR$^+$- or HCR$^-$-containing TADs in response to exposure to Pg or E2 (Fig. 5C; see also Methods section) and observed that HCR$^-$ was associated with E2-stimulated but Pg-repressed activities, as in the case of the *ESR1*- or *PGR*-TADs. In contrast, both Pg and E2 appeared to enhance the transcriptional activity of TADs containing HCR$^+$ (Fig. 5C). These opposite effects of E2 and Pg on HCR$^-$ were confirmed when we considered more specifically the enrichment of significantly hormone-regulated protein-coding genes located within HCR-containing TADs (Fig. 5D).

To explore potential associated structural changes, we analyzed at high resolution how the organization of the HCR$^-$-containing *ESR1*-TAD was modified in T47D cells exposed or not to Pg or E2 for 60 min using the enrichment

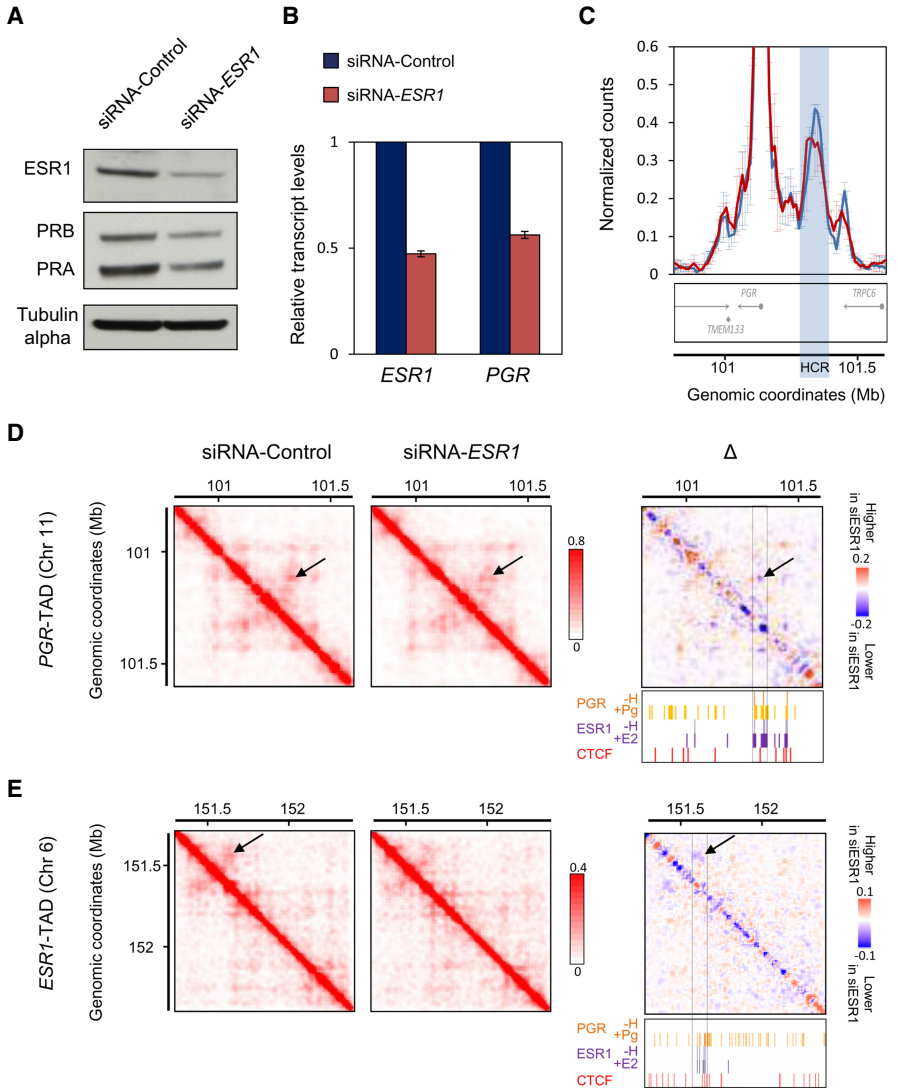

Figure 4. (*A*) Western blot showing the levels of ESR1 (p66) and PGR (PRA and PRB) observed in T47D cells transfected with scrambled siRNA (siRNA-Control) or siRNA against *ESR1* (siRNA-*ESR1*). Tubulin alpha (Antibody: Sigma, T9026) was used as loading control. The same antibodies against PGR and ESR1 were used for western blots and for ChIP experiments. (*B*) Relative levels of *ESR1* and *PGR* transcripts (average ± SD of two independent transient transfections). (*C*) Virtual 4C profiles at 10-kb resolution using the TSS of *PGR* as bait in T47D siRNA-Control cells (blue line) or siRNA-*ESR1* cells (red line) grown in the absence of hormones (average ± SD of two independent transient transfections). (*D*,*E*) Normalized in situ Hi-C contact matrices at 10-kb resolution over the *PGR*-TAD (*D*; Chr 11: 100,800,000–101,600,000) and *ESR1*-TAD (*E*; Chr 6: 151,300,000–152,400,000; *left* panels) obtained in T47D siRNA-Control cells or in siRNA-*ESR1* cells grown in the absence of hormones. The difference between the contact matrices is shown with blue and red corresponding to contacts higher and lower in T47D siRNA-Control than in T47D siRNA-*ESR1*, respectively. Arrows highlight the loops between HCRs and promoters observed in T47D cells. Position of CTCF, ESR1, and PGR binding sites in presence or absence of hormones (–H, +Pg, +E2) are shown at the *bottom* of the differential maps.

probes described in Figure 1A. In independent experiments of Chromosome conformation capture (3C) and Capture Hi-C (Supplemental Table S1), we observed opposite effects of the two hormones on the internal organization of the *ESR1*-TAD (Supplemental Fig. S7B). We pooled these capture data sets and performed differential analysis of the contact maps before/after exposure to the hormones. These comparisons demonstrated differential hormone-induced reorganization of the HCR contacts: *ESR1*-TAD HCR$^-$ interactions with promoters increased upon E2 exposure but decreased in response to Pg (Fig. 5E, top and bottom, respectively). These opposite effects were confirmed after 180 min of exposure to the hormones (Supplemental Fig. S7B). Thus, the *ESR1*-TAD HCR$^-$ acts as an enhancer in absence of hormone when ESR1 is already bound in a ligand-independent manner and its contacts with promoters are further enhanced upon exposure to E2. In contrast, upon exposure to Pg, binding of PGR to the HCR$^-$ decreased its activity, leading to a destabilization of the TAD structure. Genome-wide analysis of in situ Hi-C performed in T47D cells exposed to Pg or E2 for 30 or 180 min confirmed that the two hormones enhance the interactions of the regulatory regions with promoters in the case of HCR$^+$-containing TADs (Fig. 5F). In contrast, whereas E2 also enhances the HCR-promoter interactions within HCR$^-$-containing TADs, Pg contributes to the destabilization of the interactions engaged by HCR$^-$ (Fig. 5F). For example, as observed in the case of the *ESR1*-TAD, the interactions engaged by the HCR$^-$ located within the *PGR*-TAD with the *PGR* promoter are enhanced upon exposure to E2 but decreased in response to Pg in correlation with the opposite activities of the hormones on the expression of the gene (Supplemental Fig. S7C,D). Since the binding of CTCF to chromatin is mostly unaffected by the hormonal treatment (Supplemental Fig. S5A), these results suggest that steroid receptors bound in absence of their cognate ligand can maintain specific interactions of large regulatory regions and that these interactions dynamically and, in some cases, differentially modify upon further binding of the ESR1 and PGR receptors in response to hormones (Fig. 6).

Discussion

Here, we report the analysis at high resolution of the internal structure of the *ESR1*-TAD, which is coordinately regulated by steroid hormones in T47D cells. We found that genes within this TAD are organized around a 90-kb region of clustered binding sites for ESR1 and PGR; we defined as a hormone-control region (HCR). In the absence of hormones, this HCR already contacts the promoters of all genes within the TAD maintaining a basal expression of the resident genes (Fig. 6). Genome-wide analysis allowed us to identify more than 200 of such putative HCRs, which, as previously described for other locus control regions (Fraser and Grosveld 1998; Li et al. 2002), organize long-range interactions with promoters within their respective TAD, as well as inter-TAD interactions between them. HCRs are characterized by enhancer-related marks and recruitment of transcription-associated proteins (RNA Pol II and

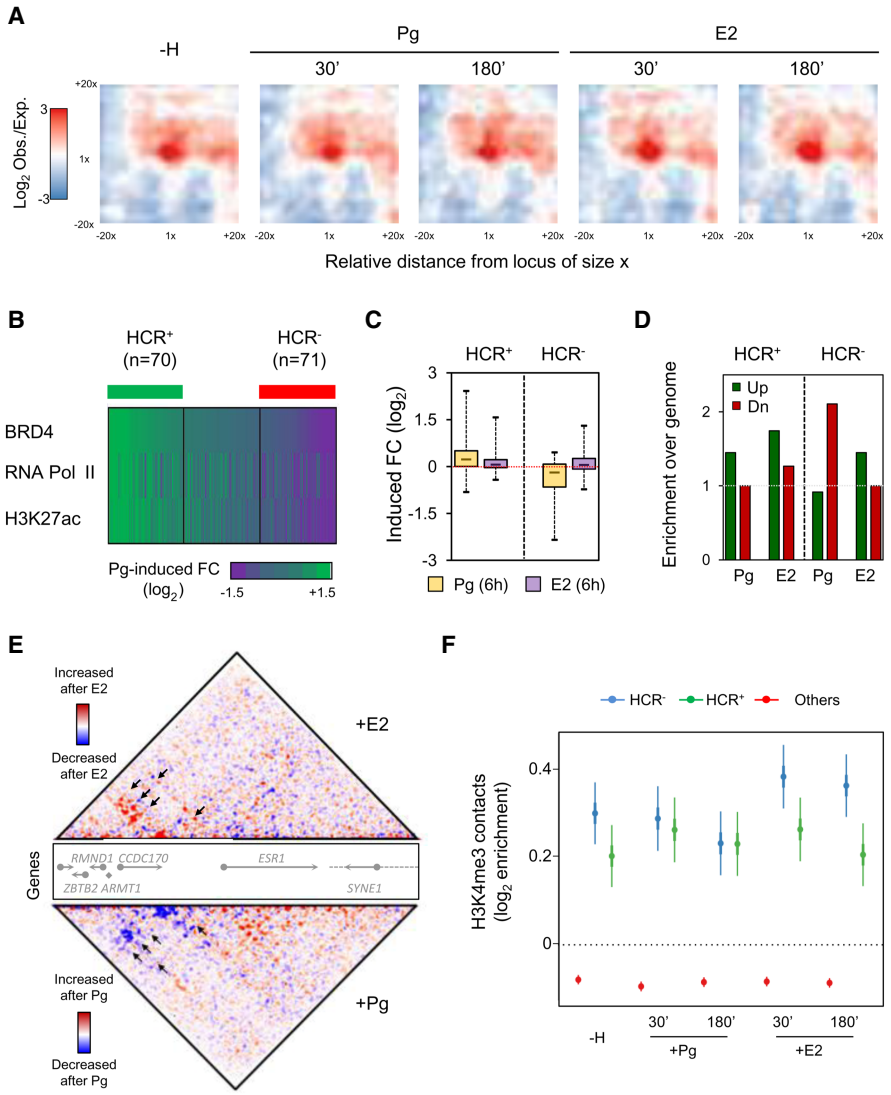

Figure 5. Hormones dynamically modify HCR-containing TAD structure and interactions. (*A*) Analysis of the long-range inter-TAD interactions established between HCRs before (as in Fig. 2F) or after 30- and 180-min exposure to Pg or E2. (*B*) Fold-change (FC) in the levels of BRD4, RNA Pol II, and H3K27ac after 30 min of treatment with Pg. Depending on the increase or decrease in BRD4 signal after exposure to Pg, we classified HCRs as HCR$^-$ or HCR$^+$, respectively (see Methods section and Supplemental Fig. S7A). (*C*) For each TAD containing a HCR$^-$ or a HCR$^+$, global changes in expression after 6 h of treatment with Pg or E2 were computed. Boxplots show the distributions of these Pg- or E2-induced fold-changes of transcripts levels per TADs. (*D*) The number of significantly up-regulated (green) or down-regulated (red) genes by Pg or E2 in TADs containing HCR$^+$ or HCR$^-$ were compared to the expected proportion of the genome. Histograms show the levels of enrichment of E2 or Pg up-regulated (green) or E2 or Pg- down-regulated (red) genes within TADs containing HCR$^+$ or HCR$^-$. (*E*) Differential analysis of the contacts obtained from Capture-C experiment on the *ESR1*-TAD before and after 60-min exposure to E2 (*top*) or Pg (*bottom*). Contacts more frequent after hormone exposure are highlighted in red, whereas contacts decreasing after hormone are labeled in blue on the heatmaps. Color key range is from −2 (blue) to +2 (red), expressed in difference of normalized contacts per million. Arrows point to the loops established between the HCR and promoters within *ESR1*-TAD. (*F*) Enrichment of intra-TAD contacts between either HCR$^+$ (green) or HCR$^-$ (blue) and H3K4me3 peaks before or after exposure to 30 and 180 min of E2 or Pg.

BRD4) in the absence of hormones and are frequently linked to genes involved in the identity of breast epithelial cells as in the case of the *ESR1*, *PGR*, and *FOXA1* genes. HCRs could therefore correspond to previously described stretch-enhancers (Parker et al. 2013) or superenhancers (Whyte et al. 2013), as in the case of the *ESR1*-TAD HCR (Hnisz et al. 2015). Indeed, it has been previously proposed that superenhancers could organize modules of integration of different signaling pathways and that perturbations of the activity of these platforms can lead to major changes in the expression of the dependent genes (Hnisz et al. 2015). In addition to support these observations, our results further demonstrate that the activity of the HCRs is highly dynamic and modular. Only 27 out of the 61 common MCF-7 and T47D HCRs have been previously classified as superenhancers in MCF-7 (Hnisz et al. 2015). This limited overlap, potentially due to lower levels of acetylated H3K27 at HCRs than at the previously identified superenhancers in MCF-7 (Hnisz et al. 2015), suggests that HCRs correspond to a specialized class of modular regulatory elements. In particular, we identified 71 of these regions where binding of the ESR1 and PGR upon exposure to the hormones in T47D cells leads to opposite effects on gene expression as well as in their contacts with the rest of the TAD (Fig. 6). We therefore suggest that these regions could act as enhancers or silencers depending on the signal received. This signal-dependent modulation of HCR activity argues not only that regulatory regions integrate various synergistic signals but that different modules can cross-talk between them in a more complex and combinatorial manner. Indeed, it appears that HCRs are complex regulatory elements spanning several tens of kilobases within which the two receptors bind at distinct sites, resulting in a fine-tuned activity of the target genes. Depending on the HCR considered, Pg and E2 can have similar effects, as exemplified by the increased levels of enhancer-associated marks and activity in response of the HCR$^+$ to E2 or Pg. In contrast, in the case of the HCR$^-$, the two hormones have opposite effects on gene expression and chromatin organization (Fig. 6). These observations therefore suggest more complex cross-talks between estrogen and progestin signaling pathways than previously described. Indeed, PGR has been proposed to be an important mediator of ER activity by modifying its landscape of binding (Mohammed et al. 2015). Our observations further show that ESR1 and PGR can bind within large genomic regulatory regions, at either overlapping or nonoverlapping sites, where the receptors can have distinct activities on gene expression.

Cell-specific intra-TAD organization, reflected by the establishment of cell-specific subdomains or chromosome neighborhoods (Phillips-Cremins et al. 2013; Dowen et al. 2014), has been proposed to depend on differential binding of architectural

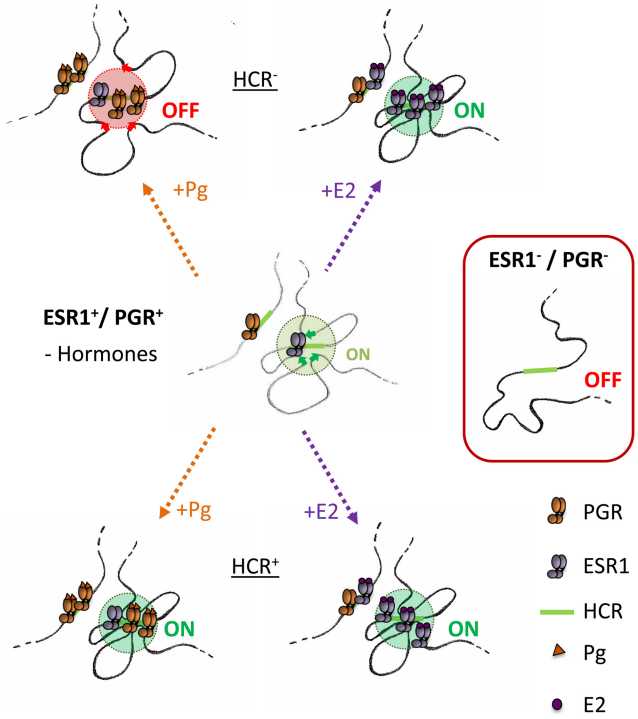

Figure 6. Dynamic organization of TADs around HCRs. HCRs correspond to regulatory regions where both ESR1 and PGR cluster after exposure to E2 or Pg. In ESR1$^+$/PGR$^-$ cells, HCRs, already occupied by unliganded receptors in the absence of hormones, organize functional loopings with promoters within the TADs and established long-range interactions between them. In the absence of receptor binding, contacts between HCRs and promoters are not established. The activity of HCR$^+$ is enhanced and the contacts between HCR$^+$ and promoters increase upon exposure to both E2 and Pg. In contrast, HCR$^-$ activity and interactions are destabilized upon binding of hormone-activated PGR, provoking a decrease in transcription of genes within the TAD, whereas exposure to E2 leads to opposing effects.

proteins like CTCF and cohesins together with subunits of the Mediator complex (Phillips-Cremins et al. 2013). The binding of CTCF remains largely similar, even between cells of different origins and of divergent ESR1 and PGR status. Differential binding of this architectural protein might therefore not be sufficient to explain the observed structural differences between these cells. In contrast, cells with divergent ESR1 and PGR status exhibit different intra-TAD organization, which correlates with the expression of the receptors and their binding at HCRs in absence of hormones. Lowering the levels of receptors in ESR1$^+$-PGR$^+$ cells leads to a destabilization of the TAD structure, pointing toward direct roles of the nuclear receptors in the organization of intra-TAD chromatin folding in the absence of hormones. It has been previously proposed that transcription factors act on a structurally preorganized context with loops between promoters and enhancers already primed prior to activation of the transcription factors (Hakim et al. 2009; Jin et al. 2013). Although the clustering of receptors is more evident after exposure to their cognate steroid hormones, our results suggest that a large fraction of HCRs is already partially occupied by the receptors, in particular by ESR1, in hormone-depleted conditions. This fraction of sites occupied by unliganded receptors might be therefore sufficient and necessary to maintain the apparent pre-established chromatin folding structure, maintaining a transcriptional memory and facilitating further response to the hormones. This highlights additional roles for steroid receptors in the absence of hormones (Vicent et al. 2013).

The fact that HCRs not only organize the 3D structure within TADs but also appear to engage long-range interactions between them suggests the existence of specific nuclear hubs where specific TADs could be enriched. Although probably highly stochastic within the cell population, these hubs of regulatory regions might serve as a reservoir of factors to facilitate transcription in a permissive environment. They may correspond to specialized transcription factories (Xu and Cook 2008) or to active hubs previously described for other steroid receptors (Hakim et al. 2011; Kuznetsova et al. 2015). Other transcription factors, for example, STAT transcription factors, have also been proposed to play a direct functional role in organizing the genome of T cells by leading to the spatial clustering of regulatory regions in specific hubs (Hakim et al. 2013) or to participate in the organization of the genome during reprogramming (Stadhouders et al. 2018).

Interactions between HCRs and promoters are further modified upon exposure to the hormones and increased binding of the receptors. This observation supports a direct role of the activated transcription factors in modifying these contacts by either reinforcing or destabilizing them. These regulatory regions can establish contacts with sites that lack actual binding sites of the receptors (e.g., *ERS1*-TAD HCR with promoters) (Fig. 1C), suggesting that the regulatory loops might be established between receptors or receptor-associated factors and other transcription factors and/or structural proteins of chromatin. Further studies will be required to properly understand how nuclear receptors facilitate the maintenance of these long-range intra-TAD contacts. In particular, it remains to be investigated whether additional transcription factors, for example, FOXA1 (Fig. 2B), also participate in establishing and/or maintaining the 3D structure of HCR-containing TADs. In addition, estrogens and progestins rapidly activate protein kinases (Vicent et al. 2006) and PARP1 (Wright et al. 2012), leading to the synthesis of nuclear ATP, which is required for the response to estrogen and progestins (Wright et al. 2016). These pathways could have important roles in the structuration of the genome, which also remains to be investigated.

In summary, we propose that in conditions where steroid hormones are depleted from the environment, a fraction of unliganded receptors, in particular ESR1, participate in the maintenance of a TAD structure that is permissive for the regulation of gene expression. Upon exposure to the hormones, further binding of the receptors can enhance or, in contrast, destabilize the interactions established between HCR and the promoters, leading to adequate response to the signals. Together, our results support a relevant role of cell-specific transcription factors in shaping the genome in a way that contributes to the integration of the cell response to external cues. It will now be important to determine how these activities are accomplished: in particular, which epigenetic factors determine the positive and negative effects of receptor recruitment to the DNA.

Methods

Cell lines and culture conditions

T47D, MCF-7, BT474, MCF10A, and SKBR3 cells were routinely grown in their optimal medium according to the ATCC recommendations. Stable T47D clones expressing shRNA empty or shRNA against *PGR* are described elsewhere (Verde et al. 2018). For RNA interference experiments, T47D cells were transiently

transfected as previously described (Nacht et al. 2016) with scramble siRNA (siRNA-Control) or siRNA directed against *ESR1* (siRNA-ESR1; sc-29305, Santa-Cruz Biotechnology). For the experiments, cells were grown 48 h in medium without phenol red complemented with 10% charcoal-dextran–treated fetal bovine serum (FBS; which corresponds to a steroid-depleted condition). After further synchronization in G0/G1 by overnight culture in medium without phenol red in absence of FBS, cells were harvested (steroid-depleted [−H] condition). In the case of hormonal treatments, cells were further treated for the times indicated with 10^{-8} M estradiol (E2) or with 10^{-8} M of the progestin analog R5020 (Pg).

ChIP and sequencing analysis

ChIP-seq experiments in T47D cells for H3K4me3, RNA-polymerase II, PGR, FOXA1, and CTCF were described previously (Ballare et al. 2013; Le Dily et al. 2014; Nacht et al. 2016). Additional ChIP-seq experiments in T47D for H3K27ac (ab4729, Abcam) and BRD4, as well as in MCF-7 for PGR (H190, Santa-Cruz Biotechnology) and ESR1 (HC20, Santa-Cruz Biotechnology), were performed as described previously (Nacht et al. 2016). After library preparation and sequencing on a HiSeq 2000, reads were trimmed and processed by aligning to the reference human genome (GRCh38) using BWA (Li and Durbin 2009). Only uniquely aligned reads were conserved. ChIP-seq signals were normalized for sequencing depth (expressed as reads per millions [rpm]), and binding sites (or peaks) were identified using MACS2 (Zhang et al. 2008).

In situ Hi-C library preparation

In situ Hi-C experiments were performed as previously described (Rao et al. 2014) with some modifications. Adherent cells were directly cross-linked on the plates with 1% formaldehyde for 10 min at room temperature. After addition of glycine (125 mM final) to stop the reaction, cells were washed with PBS and recovered by scrapping. Cross-linked cells were incubated 30 min on ice in 3C lysis buffer (10 mM Tris-HCl at pH 8, 10 mM NaCl, 0.2% NP-40, 1× anti-protease cocktail), centrifuged 5 min at 3000 rpm, and resuspended in 190 µL of NEBuffer2 1× (New England BioLabs [NEB]). Ten microliters of 10% SDS were added, and cells were incubated for 10 min at 65°C. After addition of Triton X-100 and 15-min incubation at 37°C, nuclei were centrifuged 5 min at 3000 rpm and resuspended in 300 µL of NEBuffer2 1×. Digestion was performed overnight using 400 U MboI restriction enzyme (NEB). To fill-in the generated ends with biotinylated-dATP, nuclei were pelleted and resuspended in fresh repair buffer 1× (1.5 µL of 10 mM dCTP, 1.5 µL of 10 mM dGTP, 1.5 µL of 10 mM dTTP, 37.5 µL of 0.4 mM Biotin-dATP, 50 U of DNA Polymerase I large [Klenow] fragment in 300 µL NEBuffer2 1×). After 45-min incubation at 37°C, nuclei were centrifuged 5 min at 3000 rpm, and ligation was performed for 4 h at 16°C using 10,000 cohesive end units of T4 DNA ligase (NEB) in 1.2 mL of ligation buffer (120 µL of 10× T4 DNA ligase buffer, 100 µL of 10% Triton X-100, 12 µL of 10 mg/mL BSA, 963 µL of H_2O). After reversion of the cross-link, DNA was purified by phenol extraction and EtOH precipitation. Purified DNA was sonicated to obtain fragments of an average size of 300–400 bp using a Bioruptor Pico (Diagenode; eight cycles; 20 sec on and 60 sec off). Three micrograms of sonicated DNA was used for library preparation. Briefly, biotinylated DNA was pulled down using 20 µL of Dynabeads MyOne T1 streptavidin beads in binding buffer (5 mM Tris-HCl at pH 7.5, 0.5 mM EDTA, 1 M NaCl). End-repair and A-tailing were performed on beads using NEBnext library preparation end-repair and A-tailing modules (NEB). Illumina adaptors were ligated, and libraries were amplified by eight cycles of PCR. Resulting Hi-C libraries were first controlled for quality by low sequencing depth on a NextSeq 500 prior to higher sequencing depth on HiSeq 2000. Two replicates of Hi-C were performed for each cell line and condition (Supplemental Table S1 summarizes the number of reads sequenced for each of the data sets presented in this study).

3C and Capture Hi-C

3C was performed according to the protocol described above for the Hi-C omitting the biotin-labeling step. One hundred twenty mer biotinylated RNA probes covering the region Chr 6: 149,450,000–153,750,000 (purchased from Agilent) were designed using the SureDesign software with the following parameters: density, 2×; masking, moderately stringent; and boosting, balanced. 3C samples were sonicated to an average size of 300–400 bp, and precapture libraries were generated using the SureSelect kit according to the manufacturer's instructions. Hybridization and post-capture library amplification were performed according to manufacturer instructions (Agilent). In the case of Capture Hi-C experiments, Hi-C libraries, generated according to the in situ protocol described above, were used as precapture libraries for the hybridization step.

Normalization of Hi-C matrices, differential analysis, and virtual 4C

Hi-C data were processed using an in-house pipeline based on TADbit (Serra et al. 2017). Reads were mapped according to a fragment-based strategy: Each side of the sequenced read was mapped in full length to the reference genome Human Dec. 2013 (GRCh38). In the case reads were not mapped when intra-read ligation sites were found, they were split. Individual split read fragments were then mapped independently. We used the TADbit filtering module to remove noninformative contacts and to create contact matrices as previously described (Serra et al. 2017). PCR duplicates were removed, and the Hi-C filters applied corresponded to potential nondigested fragments (extra-dangling ends), nonligated fragments (dangling-ends), self-circles, and random breaks (Supplemental Table S1 summarizes the number of reads mapped and the number of valid pairs for the different samples used in this study). The matrices obtained were normalized for sequencing depth and genomic biases using OneD (Vidal et al. 2018) and were further smoothed using a focal (moving window) average of one bin. In situ Hi-C data for GM12878 cells were obtained from Rao et al. (2014) and reprocessed as mentioned above. In Figure 1, A and B, normalized reads are expressed as normalized counts per million of genome-wide valid pairs. In the rest of the analysis, since the cell lines used are aneuploid and present different number of copies of the chromosomes analyzed, the matrices obtained in the different cell lines or conditions were further normalized for local coverage within the region (expressed as normalized counts per thousands within the region) without any correction for the diagonal decay. For differential analysis, the resulting normalized matrices were directly subtracted from each other. Virtual 4C plots were generated from these normalized matrices and correspond to histogram representation of the lines of the matrices containing the baits (therefore expressed as counts per thousand of normalized reads within the region depicted).

Genome-wide identification and classification of receptor clusters

Genomic clusters of ESR1 and/or PGR were determined by using ChIP-seq data of ESR1 and PGR in T47D or MCF-7 exposed 30 min to E2 or Pg, respectively. Binding sites for any of the two receptors (q-value $<10^{-6}$) separated by <25 kb were aggregated. Since

observing more than three binding sites for PGR or ESR1 in such window sizes was observed more frequently than expected for a random distribution (Supplemental Fig. S2A), we classified receptor clusters as follows: ESR1-clusters were regions with ESR1 binding sites of three or more and PGR binding sites of less than three; PGR-clusters were regions with PGR binding sites of three or more and ESR1 binding sites of less than three; HCRs correspond to regions with ESR1 binding sites of three or more and PGR binding sites of three or more (see Supplemental Fig. S2A). HCRs were further split as HCR^+ or HCR^- based on the average ratio of the BRD4 ChIP-seq signal within the region after/before exposure to Pg from two independent ChIP-seq experiments (HCR^+: FC > 1.1 ; HCR^-: FC < 0.9).

Intra-TAD contacts between HCRs and H3K4me3 sites

By using Hi-C matrices at 5-kb resolution, we focused on TADs containing HCRs. Each bin was labeled as part of a HCR or marked by H3K4me3 peaks or others if they did not belong to previous types. Then we gathered the observed contacts between the different types of bins within their TAD and computed expected contacts frequencies based on the genomic distance that separate each pair (the expected distance decay was calculated excluding entries outside TADs). Results are expressed as Log_2 of the ratio observed on expected frequencies of contacts.

Inter-TAD contacts between HCRs

For each intra-chromosomal pair of HCRs separated by >2 Mb, local contact matrices centered on both HCRs were generated. Since HCRs have different sizes, the matrices were generated considering bins of the size *x* of the HCR and extended upstream and downstream by 20 bins of size *x* (relative distance to HCR). The observed contacts obtained were corrected for the expected contacts in the case of random regions of similar sizes and separated by the same genomic distance. For each cell line, we excluded the local matrices of regions presenting internal copy number variations in the regions considered. The matrices were smoothed using a focal (moving window) average of one bin and cumulated to generate the meta-contact matrices.

RNA-seq

Replicate of RNA-seq experiments were performed in T47D cells treated or not with 10^{-8} M R5020 or 10^{-8} M E2 during 6 h as described previously (Le Dily et al. 2014). Together with previously published RNA-seq replicates in these cells (Le Dily et al. 2014), paired end reads were (re)mapped to the GRCh38 assembly version of the human genome with GENCODE Release 24 annotation.

Hormone-induced transcriptional changes and enrichment of regulated genes in HCR-containing TADs

A consensus list of TAD coordinates was generated based on the in situ Hi-C data sets from T47D cells with the assumption that the majority of the boundaries are comparable between cell types and upon different conditions of culture (Dixon et al. 2012; Le Dily et al. 2014). The HCRs identified in T47D were assigned to a single TAD, and TADs were classified as HCR^+ or HCR^- containing. The total RNA-seq rpm per TAD in cells treated or not with hormones was computed, and we calculated the ratio of changes per TAD as previously described (Le Dily et al. 2014). In addition, we computed the total number of genes significantly regulated by the hormones (*P*-value <0.05; |FC| > 1.5) within HCR-containing TADs and compared this observed number to the one expected based on the genome-wide proportions of responsive genes.

Data access

The raw sequencing data from this study (Hi-C, ChIP-seq, and RNA-seq) have been submitted to the NCBI Gene Expression Omnibus (GEO; http://www.ncbi.nlm.nih.gov/geo/) under accession number GSE109229.

Acknowledgments

We thank the CRG Ultra-sequencing Facility for technical support and all members of the Chromatin and Gene Expression group for helpful discussions. We acknowledge the members of the 4DGenome project (CRG and CNAG-CRG, Barcelona), notably Thomas Graf, Marc A. Marti-Renom, and Guillaume Filion, as well as Ramon Amat (UPF, Barcelona) for their helpful comments on the manuscript. We thank Dr. Cheng-Ming Chiang (UT Southwestern Medical Center) for kindly providing antibody against BRD4. We received funding from the European Research Council under the European Union's Seventh Framework Program (FP7/2007–2013)/ERC Synergy grant agreement 609989 (4DGenome). The content of this manuscript reflects only the author's views and the Union is not liable for any use that may be made of the information contained therein. We acknowledge support of the Spanish Ministry of Economy and Competitiveness, 'Centro de Excelencia Severo Ochoa 2013–2017' and Plan Nacional (SAF2016-75006-P), as well as support of the CERCA Programme/Generalitat de Catalunya.

Author contributions: F.L.D. and M.B. designed the study; F.L.D. performed most of the experiments with the help of Y.C.; G.P.V., A.S.N., P.S., R.F., and L.I.D.L. performed some ChIP-seq experiments; F.L.D. and E.V. carried out the data analysis with contributions of J.Q., J.C.-C., and J.L.V.-C.; G.V. isolated the shPGR cells; R.H.G.W. contributed to figures editing. All authors discussed the results; F.L.D. and M.B. wrote the manuscript.

References

Bain DL, Heneghan AF, Connaghan-Jones KD, Miura MT. 2007. Nuclear receptor structure: implications for function. *Annu Rev Physiol* **69:** 201–220. doi:10.1146/annurev.physiol.69.031905.160308

Ballare C, Castellano G, Gaveglia L, Althammer S, Gonzalez-Vallinas J, Eyras E, Le Dily F, Zaurin R, Soronellas D, Vicent GP, et al. 2013. Nucleosome-driven transcription factor binding and gene regulation. *Mol Cell* **49:** 67–79. doi:10.1016/j.molcel.2012.10.019

Carroll JS, Liu XS, Brodsky AS, Li W, Meyer CA, Szary AJ, Eeckhoute J, Shao W, Hestermann EV, Geistlinger TR, et al. 2005. Chromosome-wide mapping of estrogen receptor binding reveals long-range regulation requiring the forkhead protein FoxA1. *Cell* **122:** 33–43. doi:10.1016/j.cell.2005.05.008

Cavalli G, Misteli T. 2013. Functional implications of genome topology. *Nat Struct Mol Biol* **20:** 290–299. doi:10.1038/nsmb.2474

Cicatiello L, Scafoglio C, Altucci L, Cancemi M, Natoli G, Facchiano A, Iazzetti G, Calogero R, Biglia N, De Bortoli M, et al. 2004. A genomic view of estrogen actions in human breast cancer cells by expression profiling of the hormone-responsive transcriptome. *J Mol Endocrinol* **32:** 719–775. doi:10.1677/jme.0.0320719

Dixon JR, Selvaraj S, Yue F, Kim A, Li Y, Shen Y, Hu M, Liu JS, Ren B. 2012. Topological domains in mammalian genomes identified by analysis of chromatin interactions. *Nature* **485:** 376–380. doi:10.1038/nature11082

Dixon JR, Jung I, Selvaraj S, Shen Y, Antosiewicz-Bourget JE, Lee AY, Ye Z, Kim A, Rajagopal N, Xie W, et al. 2015. Chromatin architecture reorganization during stem cell differentiation. *Nature* **518:** 331–336. doi:10.1038/nature14222

Dowen JM, Fan ZP, Hnisz D, Ren G, Abraham BJ, Zhang LN, Weintraub AS, Schujiers J, Lee TI, Zhao K, et al. 2014. Control of cell identity genes occurs in insulated neighborhoods in mammalian chromosomes. *Cell* **159:** 374–387. doi:10.1016/j.cell.2014.09.030

Fraser P, Grosveld F. 1998. Locus control regions, chromatin activation and transcription. *Curr Opin Cell Biol* **10:** 361–365. doi:10.1016/S0955-0674(98)80012-4

Fraser J, Williamson I, Bickmore WA, Dostie J. 2015. An overview of genome organization and how we got there: from FISH to Hi-C. *Microbiol Mol Biol Rev* **79:** 347–372. doi:10.1128/MMBR.00006-15

Gibcus JH, Dekker J. 2013. The hierarchy of the 3D genome. *Mol Cell* **49:** 773–782. doi:10.1016/j.molcel.2013.02.011

Hakim O, John S, Ling JQ, Biddie SC, Hoffman AR, Hager GL. 2009. Glucocorticoid receptor activation of the *Ciz1-Lcn2* locus by long range interactions. *J Biol Chem* **284:** 6048–6052. doi:10.1074/jbc.C800212200

Hakim O, Sung MH, Voss TC, Splinter E, John S, Sabo PJ, Thurman RE, Stamatoyannopoulos JA, de Laat W, Hager GL. 2011. Diverse gene reprogramming events occur in the same spatial clusters of distal regulatory elements. *Genome Res* **21:** 697–706. doi:10.1101/gr.111153.110

Hakim O, Sung MH, Nakayamada S, Voss TC, Baek S, Hager GL. 2013. Spatial congregation of STAT binding directs selective nuclear architecture during T-cell functional differentiation. *Genome Res* **23:** 462–472. doi:10.1101/gr.147652.112

Hnisz D, Schuijers J, Lin CY, Weintraub AS, Abraham BJ, Lee TI, Bradner JE, Young RA. 2015. Convergence of developmental and oncogenic signaling pathways at transcriptional super-enhancers. *Mol Cell* **58:** 362–370. doi:10.1016/j.molcel.2015.02.014

Hou C, Li L, Qin ZS, Corces VG. 2012. Gene density, transcription, and insulators contribute to the partition of the *Drosophila* genome into physical domains. *Mol Cell* **48:** 471–484. doi:10.1016/j.molcel.2012.08.031

Hsu PY, Hsu HK, Singer GA, Yan PS, Rodriguez BA, Liu JC, Weng YI, Deatherage DE, Chen Z, Pereira JS, et al. 2010. Estrogen-mediated epigenetic repression of large chromosomal regions through DNA looping. *Genome Res* **20:** 733–744. doi:10.1101/gr.101923.109

Ji X, Dadon DB, Powell BE, Fan ZP, Borges-Rivera D, Shachar S, Weintraub AS, Hnisz D, Pegoraro G, Lee TI, et al. 2016. 3D chromosome regulatory landscape of human pluripotent cells. *Cell Stem Cell* **18:** 262–275. doi:10.1016/j.stem.2015.11.007

Jin F, Li Y, Dixon JR, Selvaraj S, Ye Z, Lee AY, Yen CA, Schmitt AD, Espinoza CA, Ren B. 2013. A high-resolution map of the three-dimensional chromatin interactome in human cells. *Nature* **503:** 290–294. doi:10.1038/nature12644

Kuznetsova T, Wang SY, Rao NA, Mandoli A, Martens JH, Rother N, Aartse A, Groh L, Janssen-Megens EM, Li G, et al. 2015. Glucocorticoid receptor and nuclear factor κ-b affect three-dimensional chromatin organization. *Genome Biol* **16:** 264. doi:10.1186/s13059-015-0832-9

Le Dily F, Bau D, Pohl A, Vicent GP, Serra F, Soronellas D, Castellano G, Wright RH, Ballare C, Filion G, et al. 2014. Distinct structural transitions of chromatin topological domains correlate with coordinated hormone-induced gene regulation. *Genes Dev* **28:** 2151–2162. doi:10.1101/gad.241422.114

Li H, Durbin R. 2009. Fast and accurate short read alignment with Burrows–Wheeler transform. *Bioinformatics* **25:** 1754–1760. doi:10.1093/bioinformatics/btp324

Li Q, Peterson KR, Fang X, Stamatoyannopoulos G. 2002. Locus control regions. *Blood* **100:** 3077–3086. doi:10.1182/blood-2002-04-1104

Li W, Notani D, Ma Q, Tanasa B, Nunez E, Chen AY, Merkurjev D, Zhang J, Ohgi K, Song X, et al. 2013. Functional roles of enhancer RNAs for oestrogen-dependent transcriptional activation. *Nature* **498:** 516–520. doi:10.1038/nature12210

Lupianez DG, Kraft K, Heinrich V, Krawitz P, Brancati F, Klopocki E, Horn D, Kayserili H, Opitz JM, Laxova R, et al. 2015. Disruptions of topological chromatin domains cause pathogenic rewiring of gene-enhancer interactions. *Cell* **161:** 1012–1025. doi:10.1016/j.cell.2015.04.004

Mohammed H, Russell IA, Stark R, Rueda OM, Hickey TE, Tarulli GA, Serandour AA, Birrell SN, Bruna A, Saadi A, et al. 2015. Progesterone receptor modulates ERα action in breast cancer. *Nature* **523:** 313–317. doi:10.1038/nature14583

Nacht AS, Pohl A, Zaurin R, Soronellas D, Quilez J, Sharma P, Wright RH, Beato M, Vicent GP. 2016. Hormone-induced repression of genes requires BRG1-mediated H1.2 deposition at target promoters. *EMBO J* **35:** 1822–1843. doi:10.15252/embj.201593260

Nora EP, Lajoie BR, Schulz EG, Giorgetti L, Okamoto I, Servant N, Piolot T, van Berkum NL, Meisig J, Sedat J, et al. 2012. Spatial partitioning of the regulatory landscape of the X-inactivation centre. *Nature* **485:** 381–385. doi:10.1038/nature11049

Parker SC, Stitzel ML, Taylor DL, Orozco JM, Erdos MR, Akiyama JA, van Bueren KL, Chines PS, Narisu N, Program NCS, et al. 2013. Chromatin stretch enhancer states drive cell-specific gene regulation and harbor human disease risk variants. *Proc Natl Acad Sci* **110:** 17921–17926. doi:10.1073/pnas.1317023110

Phillips-Cremins JE, Sauria ME, Sanyal A, Gerasimova TI, Lajoie BR, Bell JS, Ong CT, Hookway TA, Guo C, Sun Y, et al. 2013. Architectural protein subclasses shape 3D organization of genomes during lineage commitment. *Cell* **153:** 1281–1295. doi:10.1016/j.cell.2013.04.053

Pope BD, Ryba T, Dileep V, Yue F, Wu W, Denas O, Vera DL, Wang Y, Hansen RS, Canfield TK, et al. 2014. Topologically associating domains are stable units of replication-timing regulation. *Nature* **515:** 402–405. doi:10.1038/nature13986

Rao SS, Huntley MH, Durand NC, Stamenova EK, Bochkov ID, Robinson JT, Sanborn AL, Machol I, Omer AD, Lander ES, et al. 2014. A 3D map of the human genome at kilobase resolution reveals principles of chromatin looping. *Cell* **159:** 1665–1680. doi:10.1016/j.cell.2014.11.021

Sanyal A, Lajoie BR, Jain G, Dekker J. 2012. The long-range interaction landscape of gene promoters. *Nature* **489:** 109–113. doi:10.1038/nature11279

Seitan VC, Faure AJ, Zhan Y, McCord RP, Lajoie BR, Ing-Simmons E, Lenhard B, Giorgetti L, Heard E, Fisher AG, et al. 2013. Cohesin-based chromatin interactions enable regulated gene expression within preexisting architectural compartments. *Genome Res* **23:** 2066–2077. doi:10.1101/gr.161620.113

Serra F, Bau D, Goodstadt M, Castillo D, Filion GJ, Marti-Renom MA. 2017. Automatic analysis and 3D-modelling of Hi-C data using TADbit reveals structural features of the fly chromatin colors. *PLoS Comput Biol* **13:** e1005665. doi:10.1371/journal.pcbi.1005665

Sexton T, Yaffe E, Kenigsberg E, Bantignies F, Leblanc B, Hoichman M, Parrinello H, Tanay A, Cavalli G. 2012. Three-dimensional folding and functional organization principles of the *Drosophila* genome. *Cell* **148:** 458–472. doi:10.1016/j.cell.2012.01.010

Stadhouders R, Vidal E, Serra F, Di Stefano B, Le Dily F, Quilez J, Gomez A, Collombet S, Berenguer C, Cuartero Y, et al. 2018. Transcription factors orchestrate dynamic interplay between genome topology and gene regulation during cell reprogramming. *Nat Genet* **50:** 238–249. doi:10.1038/s41588-017-0030-7

Verde G, De Llobet LI, Wright RHG, Quilez J, Peiró S, Le Dily F, Beato M. 2018. Unliganded progesterone receptor governs estrogen receptor gene expression by regulating DNA methylation in breast cancer cells. *Cancers* **10:** 371. doi:10.3390/cancers10100371

Vicent GP, Ballare C, Nacht AS, Clausell J, Subtil-Rodriguez A, Quiles I, Jordan A, Beato M. 2006. Induction of progesterone target genes requires activation of Erk and Msk kinases and phosphorylation of histone H3. *Mol Cell* **24:** 367–381. doi:10.1016/j.molcel.2006.10.011

Vicent GP, Nacht AS, Zaurin R, Font-Mateu J, Soronellas D, Le Dily F, Reyes D, Beato M. 2013. Unliganded progesterone receptor-mediated targeting of an RNA-containing repressive complex silences a subset of hormone-inducible genes. *Genes Dev* **27:** 1179–1197. doi:10.1101/gad.215293.113

Vidal E, le Dily F, Quilez J, Stadhouders R, Cuartero Y, Graf T, Marti-Renom MA, Beato M, Filion GJ. 2018. OneD: increasing reproducibility of Hi-C samples with abnormal karyotypes. *Nucleic Acids Res* **46:** e49. doi:10.1093/nar/gky064

Whyte WA, Orlando DA, Hnisz D, Abraham BJ, Lin CY, Kagey MH, Rahl PB, Lee TI, Young RA. 2013. Master transcription factors and mediator establish super-enhancers at key cell identity genes. *Cell* **153:** 307–319. doi:10.1016/j.cell.2013.03.035

Wright RH, Castellano G, Bonet J, Le Dily F, Font-Mateu J, Ballare C, Nacht AS, Soronellas D, Oliva B, Beato M. 2012. CDK2-dependent activation of PARP-1 is required for hormonal gene regulation in breast cancer cells. *Genes Dev* **26:** 1972–1983. doi:10.1101/gad.193193.112

Wright RH, Lioutas A, Le Dily F, Soronellas D, Pohl A, Bonet J, Nacht AS, Samino S, Font-Mateu J, Vicent GP, et al. 2016. ADP-ribose–derived nuclear ATP synthesis by NUDIX5 is required for chromatin remodeling. *Science* **352:** 1221–1225. doi:10.1126/science.aad9335

Xu M, Cook PR. 2008. Similar active genes cluster in specialized transcription factories. *J Cell Biol* **181:** 615–623. doi:10.1083/jcb.200710053

Zhan Y, Mariani L, Barozzi I, Schulz EG, Blüthgen N, Stadler M, Tiana G, Giorgetti L. 2017. Reciprocal insulation analysis of Hi-C data shows that TADs represent a functionally but not structurally privileged scale in the hierarchical folding of chromosomes. *Genome Res* **27:** 479–490. doi:10.1101/gr.212803.116

Zhang Y, Liu T, Meyer CA, Eeckhoute J, Johnson DS, Bernstein BE, Nusbaum C, Myers RM, Brown M, Li W, et al. 2008. Model-based Analysis of ChIP-Seq (MACS). *Genome Biol* **9:** R137. doi:10.1186/gb-2008-9-9-r137

Received September 14, 2018; accepted in revised form November 15, 2018.

Hormone-control regions mediate steroid receptor–dependent genome organization

François Le Dily, Enrique Vidal, Yasmina Cuartero, et al.

Genome Res. published online December 14, 2018
Access the most recent version at doi:10.1101/gr.243824.118